NASA TECHNICAL
MEMORANDUM

NASA TM X-64604

WIND BIASING TECHNIQUES FOR USE IN OBTAINING LOAD RELIEF

By Gale Ernsberger
Aero-Astrodynamics Laboratory

June 14, 1971

NASA

George C. Marshall Space Flight Center
Marshall Space Flight Center, Alabama

TECHNICAL REPORT STANDARD TITLE PAGE

1. REPORT NO.	2. GOVERNMENT ACCESSION NO.	3. RECIPIENT'S CATALOG NO.
NASA TM X-64604		

4. TITLE AND SUBTITLE	5. REPORT DATE
WIND BIASING TECHNIQUES FOR USE IN OBTAINING LOAD RELIEF	June 14, 1971
	6. PERFORMING ORGANIZATION CODE
7. AUTHOR(S)	8. PERFORMING ORGANIZATION REPORT #
Gale Ernsberger	
9. PERFORMING ORGANIZATION NAME AND ADDRESS	10. WORK UNIT NO.
George C. Marshall Space Flight Center Marshall Space Flight Center, Alabama 35812	11. CONTRACT OR GRANT NO.
	13. TYPE OF REPORT & PERIOD COVERED
12. SPONSORING AGENCY NAME AND ADDRESS	TECHNICAL MEMORANDUM
NASA Washington, D. C. 20546	14. SPONSORING AGENCY CODE

15. SUPPLEMENTARY NOTES

16. ABSTRACT

The techniques used in wind biasing to obtain load relief are discussed in detail. The merits of biasing to various statistical wind models are discussed with emphasis placed on the monthly mean vector wind. Substantial load relief is demonstrated for the AAP-1 Skylab launch vehicle by biasing in both pitch and yaw. The advantages of hybrid computer simulations with Jimsphere wind profile inputs are discussed. Comparisons between launch delay risk using the synthetic wind approach and the Jimsphere detailed wind show that the detail wind gives a more realistic approach and a lower launch delay risk.

17. KEY WORDS	18. DISTRIBUTION STATEMENT
Skylab, Vehicle Dynamics, Wind Biasing, Detail Wind, Load Relief, Probability Statements	FOR PUBLIC RELEASE: for E. D. Geissler Director, Aero-Astrodynamics Laboratory

19. SECURITY CLASSIF. (of this report)	20. SECURITY CLASSIF. (of this page)	21. NO. OF PAGES	22. PRICE
UNCLASSIFIED	UNCLASSIFIED	37	$3.00

MSFC - Form 3292 (May 1969)

TABLE OF CONTENTS

LIST OF ILLUSTRATIONS

LIST OF ILLUSTRATIONS (Continued)

WIND BIASING TECHNIQUES FOR USE IN OBTAINING LOAD RELIEF

I. INTRODUCTION

The AAP-1 Skylab launch vehicle with the Saturn S-IC and S-II boost stages has exhibited reduced launch capability due to high altitude winds as compared to other Saturn class vehicles. The configuration is such that the vehicle has a lower control moment and a higher aerodynamic moment, resulting in large vehicle loads. The changes in the configuration forward of the S-IVB stage have also reduced the structural capability. The increase in vehicle loads coupled with the decreased structural capability has resulted in a lower launch probability during months with predominantly high wind magnitudes and/or high wind shears.

Load relief in aerodynamically unstable vehicles is usually accomplished by implementing a load relief control system, by wind biasing, or by a combination of the two methods. Since the Skylab control system utilizes the existing Saturn V hardware, it has a fixed control scheme employing rate sensors and attitude error feedback. The Saturn V has no provisions for accelerometer or angle-of-attack feedback to provide load relief. Since the booster is already built, there is no possibility of increasing the size of the fins, etc., to reduce the amount of aerodynamic instability.

The only remaining avenue of approach then is through wind biasing. This is a load relief technique wherein the trajectory is shaped to cause the vehicle to fly a prescribed angle-of-attack profile (usually zero) in the presence of the biasing wind profile during the high dynamic pressure region of flight. Wind biasing is not a new approach for Saturn vehicles since the Saturn I, IB, and V have all used wind biasing for various reasons, generally, to provide additional load relief and minimize drift. Saturn SA-6 was an exception in that the biasing was done to induce a four-degree angle of attack to provide a good assessment of the aerodynamic characteristics and structural capability.

Initial attempts to provide a wind-biased trajectory for the Skylab vehicle indicated a number of contradictory trends, mainly that the vehicle would not fly the biasing steady-state wind when subjected to design shears and gusts. Subsequently, the entire procedure of wind biasing, analysis of vehicle uncertainties (thrust misalignment, c.g. offset, etc.), evaluation of wind limits, and even the wind statistics were examined (see Section IV).

The Skylab was originally planned to fly along an azimuth of 63°. This flight azimuth would have required only a nominal pitch plane bias. However, the decision to go to a 45° flight azimuth required a significantly different type of biasing. The predominant west-to-east winds of the Eastern Test Range (ETR) are tailwinds for easterly launch azimuths, but for the 45° azimuth, they become a combination of tail- and left cross-wind. Since the mean tail- and cross-wind magnitudes are approximately equal, biasing in pitch and yaw simultaneously was recommended. This is discussed further in Section IV.

The basic procedures followed on previous Saturn vehicles were used to assess the structural capability. These procedures are described in detail in the following section.

The author wishes to express his appreciation to Mr. Zachary Galaboff for his efforts in programming the mathematical model and for assistance in obtaining results. Thanks are also due Mr. Randy Steinberg for aid in running the program and plotting the preliminary results.

II. ASSESSMENT OF STRUCTURAL CAPABILITY

In the past, the structural capability of Saturn vehicles has been assessed in terms of wind limits. Beginning with a set of nominal vehicle wind response data, rigid body structural limits have been generated. These data are furnished as a limiting envelope of bending moment capability for various flight times (or Mach number ranges). These envelopes are then used to assess the vehicle's maximum wind magnitude capability.

Next, the vehicle data uncertainties are assessed to reflect the 3σ level of confidence in the best estimate available. These variations include, but are not necessarily limited to, the following:

(1) normal force coefficient - C_N

(2) center of pressure - C_P

(3) center of gravity

(4) control gains

(5) mass and/or thrust

(6) thrust vector misalignment of fixed and control engines, etc.

These uncertainties are combined in such a manner as to increase the vehicle bending moment to a maximum. The procedure is simplified somewhat by root-sum-squaring individual contributions to major uncertainties. For example, the thrust vector misalignment of the control engine is composed of uncertainties due to vehicle manufacturing and assembly procedures (tolerance buildup, stacking errors, etc.), as well as those due to null offsets in the electronic components, sensors, etc. The individual uncertainties are combined statistically to give the effective misalignment of the thrust vector.

The vehicle is then modeled and flown (simulated) through a family of synthetic wind profiles containing shears and gusts constructed in accordance with reference 1. The profiles are constructed to peak at a range of altitudes, typically 8, 10, and 12 km, corresponding to the maximum dynamic pressure (max q) region of boost flight. The data uncertainties are incorporated to produce the maximum α's and β's for these profiles. The steady-state wind value which produces a value of bending moment equal to the limit bending moment capability becomes the wind limit for that given altitude. The process is repeated to provide a limit at each altitude for head, tail, and left and right cross-winds.

These wind limits (or envelopes of capability) are then used in a counting procedure to determine the number of wind profiles from a sample of the entire population of winds which fall inside and outside of the limits. This then allows the analyst to compute the probability of success (or failure). Since the joint probability of these steady-state vector wind magnitudes and shears was not known until recently (reference 2), only a scalar "conditional" probability statement could be made for the launch. By conditional we mean "for a specified altitude, given that non-nominal vehicle parameters occur and given that the 99% scalar wind shear and gusts occur, the critical wind speed occurs at the specified altitude." Then the probability of a launch success (or failure) is a determinable percentage. While the entire procedure is somewhat conservative, earlier Saturn boosters had sufficient capability to permit this procedure to be used.

The same procedure was used successfully to evaluate the capability for both wind-biased and nonbiased trajectories. One serious difficulty with the biasing procedure was encountered, however, in evaluating the wind limits for Skylab. Load limits were exceeded for synthetic wind profiles with steady-state wind magnitudes about equal to the expected or mean wind. After careful analysis of the problem, it was determined that the plane of symmetry of vehicle capability was rotated as well as translated by the bias. By introducing synthetic winds as directional winds in 45-degree increments, a better definition of the envelope of capability was obtained. However, since the wind shear increases as the steady-state magnitude increases, any large gain in structural capability due to biasing tended to be negated.

Adding the 3σ data uncertainties in the worst direction further reduced launch probability. A more reasonable treatment of the data uncertainties is to obtain the root-sum-square (RSS) of the individual perturbation effects. The "A" factor method of reference 3 is a technique by which the data uncertainties can be combined to obtain the desired RSS effect in one computer run after the initial analysis of the perturbation solutions. The perturbation factor "A" is calculated as follows:

$$A = \frac{\left(\sum_{i=1}^{n} \Delta M_{B_i}^2\right)^{1/2}}{\Delta M_{B_{max}}}, \qquad (1)$$

where

ΔM_{B_i} = (bending moment for ith perturbation) - (nominal bending moment)

and

$\Delta M_{B_{max}}$ = (bending moment for all perturbations simultaneously in worst direction) - (nominal bending moment).

Alternately,

$$\Delta M_{B_{max}} \sim \sum_{i=1}^{n} \Delta M_{B_i}. \qquad (2)$$

The "A" factor is then used as a scale factor to reduce the independent 3σ uncertainties to an approximate 3σ combined probability of occurrence. The "A" factor generally varies between 0.4 and 0.6 being dependent on altitude, as well as on vehicle station. A value of 0.5 has been found to provide satisfactory results for preliminary analyses. Since the number of runs to be considered is large, a more accurate value can be determined after preliminary analyses are completed. Also, because of the nonlinear nature of the effects of the uncertainties on the vehicle performance, several trial values may be required to find the "A" factor which gives the RSS value of bending moment.

However, even by using this procedure in the analysis, the Skylab vehicle was found to have a low launch probability. In order to increase the launch probability, wind-biasing techniques were investigated to determine whether a different approach could be used.

III. TECHNIQUES FOR WIND BIASING

To gain an understanding of wind biasing approaches, biasing in only one plane (yaw) was analyzed. The pitch plane can be treated in the same manner as a perturbation about a nominal gravity turn. The linearized expression for the total angle of attack (α_T) in one plane (yaw) is

$$\alpha_T = \varphi + \frac{V_W}{V} - \frac{\dot{Y}}{V} \tag{3}$$

= (vehicle attitude) + (wind angle of attack)

- (drift induced angle of attack).

For a given wind profile, the parameters which can be controlled to reduce the total angle of attack α_T of (3) are φ and $\dot{Y}$.

To minimize α_T, one could continuously control (steer) the vehicle into the wind such that

$$\varphi = (\dot{Y} - V_W)/V. \tag{4}$$

The vehicle is simply commanded to align its longitudinal axis along the relative velocity vector.

The vehicle may also be steered such that φ is set equal to zero and the drift rate ($\dot{Y}$) is equal to the wind velocity (V_W). Another choice would be to balance part of the angle of attack with drift rate in the maximum dynamic pressure (max q) region of flight and the remainder by turning into the wind. This is the present technique used on Saturn launch vehicles and can be tailored to minimize terminal drift as well as angle-of-attack during max q. Several choices exist for the proper balance between vehicle drift and turning into the wind. These choices are explored in the following sections, along with a discussion of the model and basic data.

A. Linearized Equations of Motion

A simplified set of equations of motion was derived for the yaw plane in accordance with the sign conventions indicated in figure 1. The resulting equations are as follows:

$\ddot{\varphi}$ = vehicle angular acceleration (5)

$= -C_1\alpha - C_2\beta$

$\ddot{\gamma}$ = vehicle lateral acceleration (6)

$= G_1\varphi + G_2\alpha + G_3\beta$

β = commanded engine deflection (7)

$= a_o\psi + a_1\dot{\varphi} + b_o\alpha$

ψ = vehicle attitude heading error (8)

$= \varphi - \chi_c$

α_T = total angle of attack (9)

$= \varphi + \frac{1}{V}(V_w - \dot{Y})$.

B. Data Base

Typical values of V, C_1, C_2, etc., were derived from Skylab data (see table 1). Nominal values of a_o and a_1 were 0.9 and 1.03, respectively. The angle of attack feedback gain b_o was nominally zero.

TABLE 1

Time (sec)	C_1 (sec^{-2})	C_2 (sec^{-2})	G_1 ($m\text{-}sec^{-2}$)	G_2 ($m\text{-}sec^{-2}$)	G_3 ($m\text{-}sec^{-2}$)	V ($m\text{-}sec^{-1}$)
20	-.013	1.08	13.5	.26	10.8	59
30	-.035	1.11	14.4	.75	11.5	100
40	-.069	1.14	15.4	1.65	12.4	151
50	-.108	1.18	16.7	3.09	13.5	214
60	-.090	1.23	18.0	5.36	14.7	291
70	-.241	1.28	19.4	6.69	16.1	381
80	-.330	1.35	21.5	6.44	17.7	495
90	-.267	1.42	23.9	4.87	19.4	645

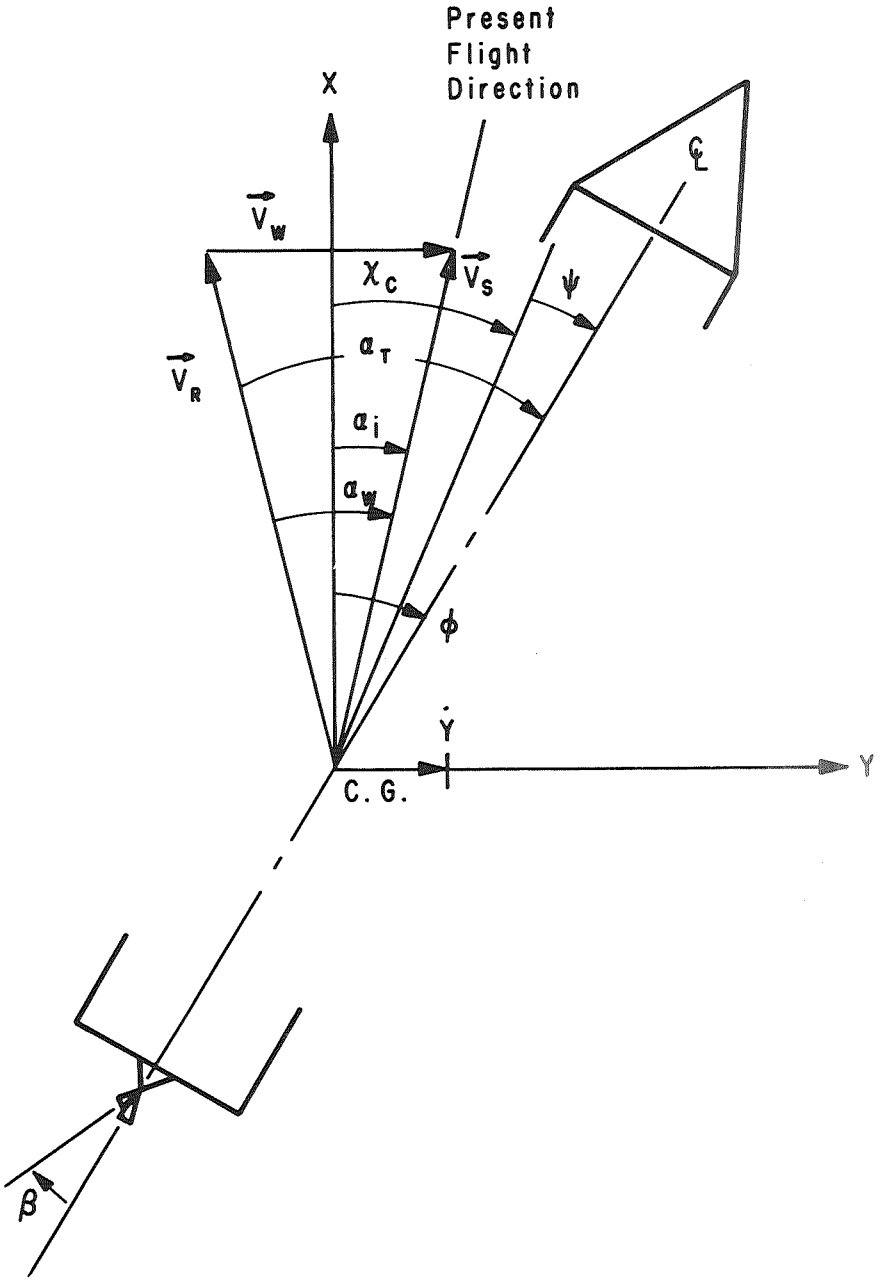

Figure 1. Rigid Body Coordinates, Yaw Plane

C. Bending Moment Indicator

To facilitate a realistic evaluation of the relative merits of each biasing technique investigated, a simplified bending moment I_B indicator for an arbitrary station was derived as follows:

$$M_T(x) = M'_\alpha(x)\ \alpha_T + M'_\beta(x)\ \beta_T \tag{10}$$

$$I_B = \frac{M_T(x)}{M'_\beta(x)} \qquad ;\quad x \leq 90 \text{ m}$$

$$= R(x)\ \alpha_T + \beta_T. \tag{11}$$

The bending moment coefficients $M'_\alpha(x)$ and $M'_\beta(x)$ each contain the moment contributions of static and inertia loads due to a unit angle of attack and engine deflection taken independently. Figure 2 shows a typical range of $M'_\alpha(x)$, $M'_\beta(x)$, and R(x) for the configuration being studied. It can be seen from (11) that as R(x) increases, the bending moment becomes insensitive to engine deflections.

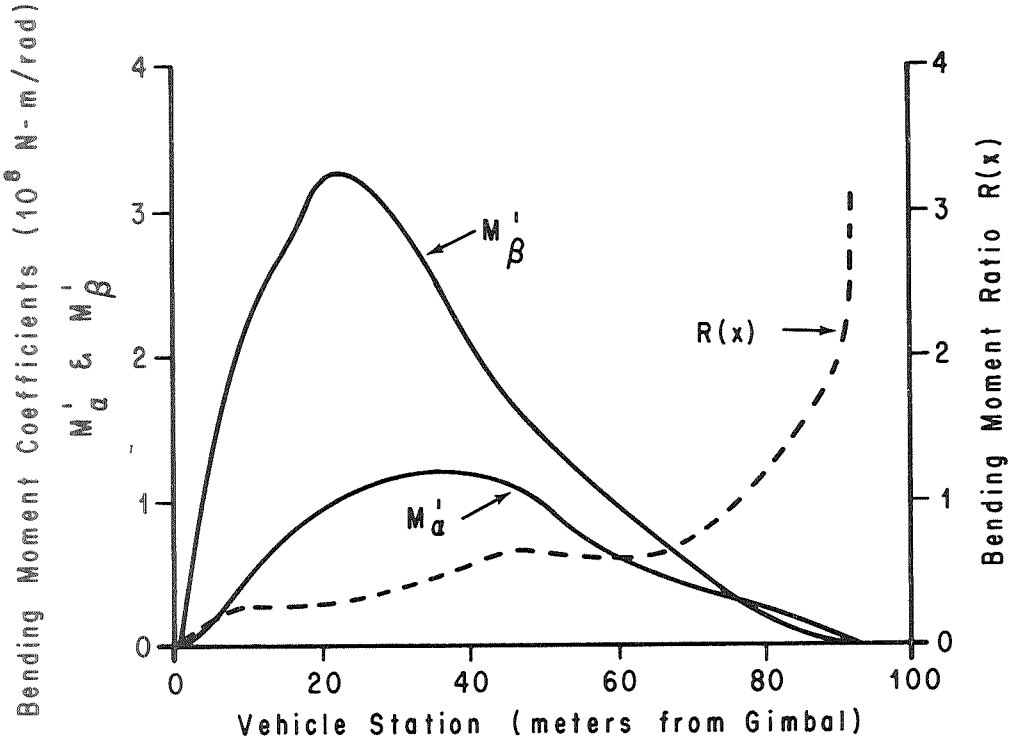

Figure 2. Typical Bending Moment Coefficients and Resulting Bending Moment Ratio

D. Basic Techniques

The technique used to generate the biasing trajectories was to set up an initial drift by setting χ_c equal to a constant over the initial portion of flight. This constant is later referred to as the initial steering ledge. In general, the vehicle drift at lower altitudes is opposite in direction to the drift at max q. At low altitudes χ_c is generated such that the vehicle turns with the wind. To force the vehicle to turn into the wind in the max q region of flight, the steering command is defined as

$$\chi_c = \frac{\dot{Y} - V_w}{V}. \tag{12}$$

This approximation assumes that φ in equation (3) is equal to χ_c if the control is perfect. The assumption is justified in that α_T was generally of the order $-0.3 \leqq \alpha_T \leqq 0.3°$. Since φ generally lags χ_c, a more realistic approach might be to let

$$\chi_c(t) = \frac{\dot{Y}(t + \Delta t) - V_w(t + \Delta t)}{V(t + \Delta t)}, \tag{13}$$

where Δt is a time differential to account for the phase lag in the control system due to nonideal effects. Since these effects were considered small based on previous Apollo vehicle studies, they were not investigated.

E. Verification of Simple Dynamic Model

In figure 3, the results of the planar model (equations (5) through (9)) are compared with the yaw steering history obtained from a complete 6-D trajectory simulation with non-ideal control to determine the accuracy of the simplified approach. The principal differences in the steering commands are attributed to control system lags not simulated in the simplified model. Both systems exhibited similar lateral drift rates using the mean wind profile as the forcing (or biasing) function. Based on the comparisons shown in figures 3 and 4, it was concluded that the simplified dynamic model was adequate for the purpose of this study.

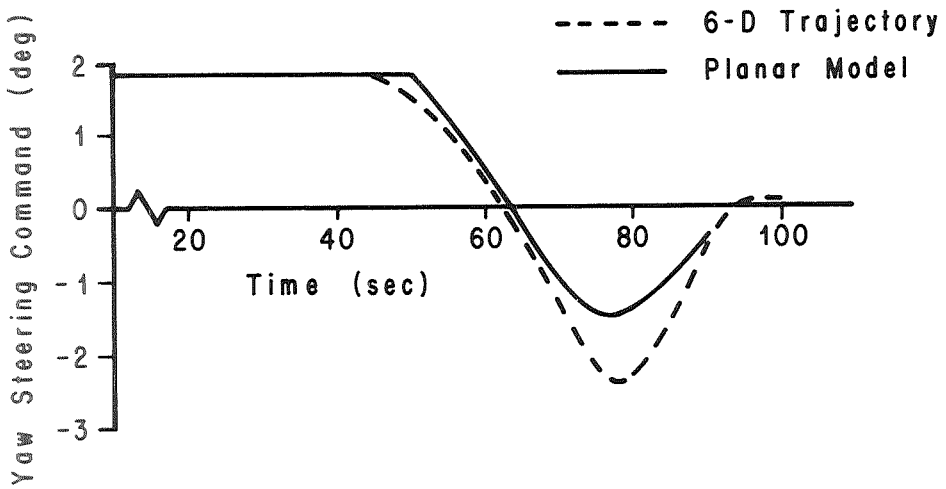

Figure 3. Comparison of Steering Commands from 6-D Trajectory Simulation and Yaw Plane Model for Mean Wind Profile

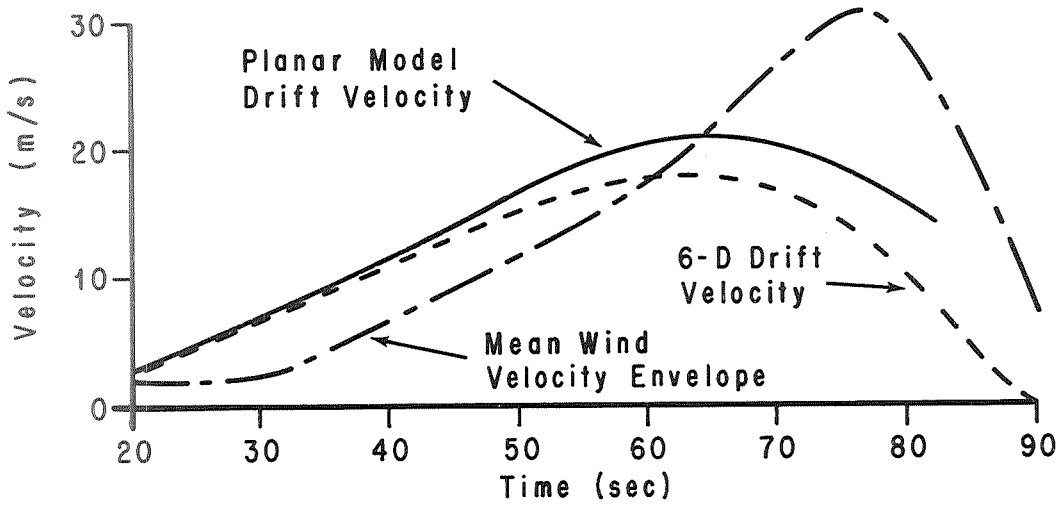

Figure 4. Comparison of Drift Rates for Planar Model and 6-D Simulation with Mean Wind Velocity Envelope

F. Basic Results

Several different approaches to developing a bias trajectory were investigated along with the trade-offs involved. These approaches are discussed in the following paragraphs.

1. Mean Wind Bias

Since the initial Skylab structural assessment using a complete 6-D simulation indicated the most severe wind restrictions (or highest vehicle loads) occur at approximately 10 km (~ 71 sec), most of the results presented are for this case. The trends can generally be applied to other altitudes. Approximate structural limits in terms of the bending moment indicator (I_b) were developed to provide a basis for comparison.

To provide a basis from comparison between the various techniques investigated in the study, the planar model bias steering command shown in figure 3 was developed for the mean yaw wind component shown in figure 4. A family of synthetic winds [1] was constructed for steady-state wind speeds of 35, 50, 60 and 70 m/sec peaking at altitudes of 8, 10 and 12 km. The variation of I_b for the 70 m/sec synthetic profile for the nonbiased and mean wind biased steering commands is shown in figure 5. Both sets of results fell outside the allowable envelope of I_b with the nonbiased steering command indicating 34% higher loads than the biased command at 10 km.

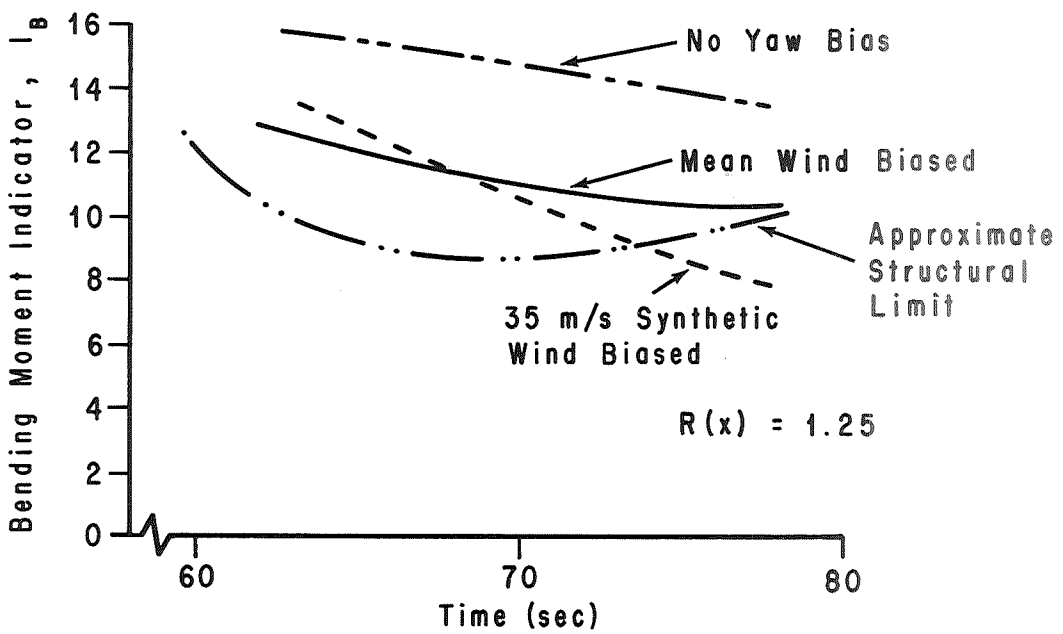

Figure 5. Bending Moment Indicator for 70 m/s Synthetic Winds Peaking at 8, 10 and 12 km (64, 70 and 75 sec)

The results obtained by plotting I_b versus steady-state wind speed for winds peaking at 10 km are shown in figure 6. When compared to the allowable value of I_b at 10 km, wind speed limits of 35 m/sec and 58 m/sec were obtained for the nonbiased and mean wind biased steering commands.

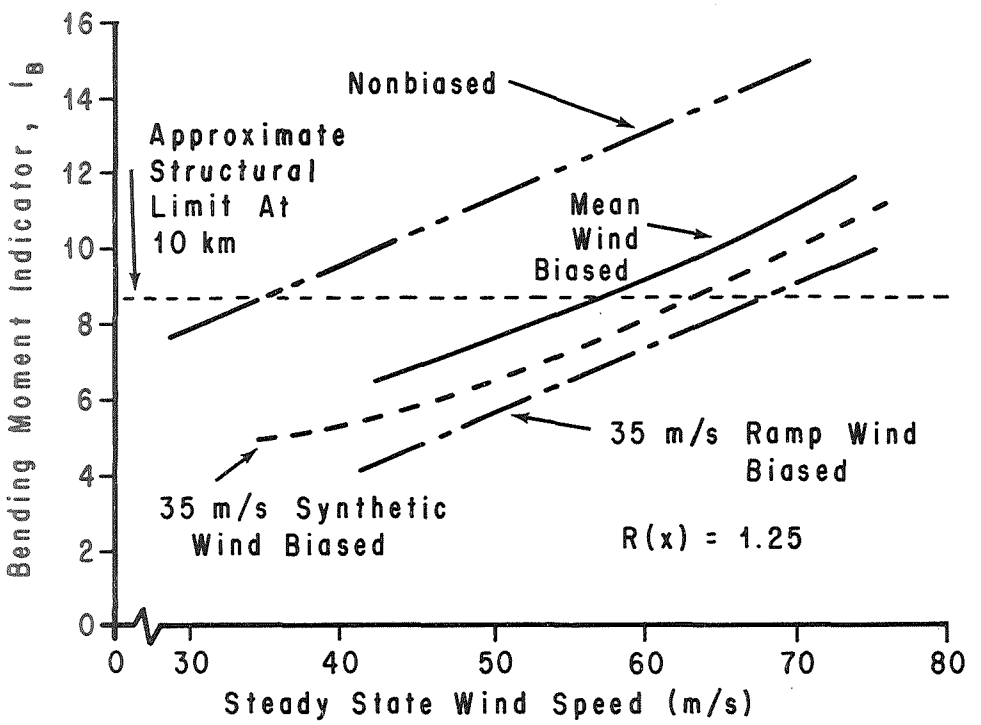

Figure 6. Results of Planar Simulation Showing Reduction in Wind Restriction for Biased and Unbiased Trajectories at 10 km

2. Shear Biasing

Some earlier 6-D simulation results showed that the Skylab vehicle could withstand a smooth wind profile with a peak wind speed of 120 m/sec (obtained by scaling up the mean wind until the vehicle capability was exceeded). These results provided a clue that the wind shear buildup might be the major contributor to the loss of capability. To assess the effects of the shear buildup, a synthetic wind with a steady-state wind speed of 35 m/sec peaking at 10 km was used as the basis for the biasing command instead of the mean wind. The 99% shears were reduced by 15% (in accordance with reference 1) with the gust omitted. Including the gust did not affect vehicle response. The results obtained using the shear biased steering command are compared with the results

obtained using nonbiased and mean wind biased commands in figures 5 and 6. There were definite improvements in capability using the shear bias at 10 and 12 km.

Figure 6 compares the results of the above three steering commands for the bending moment indicator at 10 km. To provide a check on the trends indicated by these results, yaw wind speed limits at 10 km were obtained from a complete 6-D simulation using these three steering commands. The 6-D simulation used a gravity turn pitch tilt with appropriate yaw bias steering command. The comparison of results is as follows:

	Planar	6-D
(1) Nonbiased (m/s)	35	36
(2) Mean Wind Biased (m/s)	58	53
(3) Synthetic Wind Biased (m/s)	63	59

As an alternate approach to establishing the base wind for shear biasing, a ramp wind roughly following the buildup of the synthetic wind was constructed. This profile has the advantage of requiring fewer points to represent the altitude variation, thus saving computer storage. Figure 7 shows a comparison of the synthetic and ramp wind profiles used for a typical altitude (10 km).

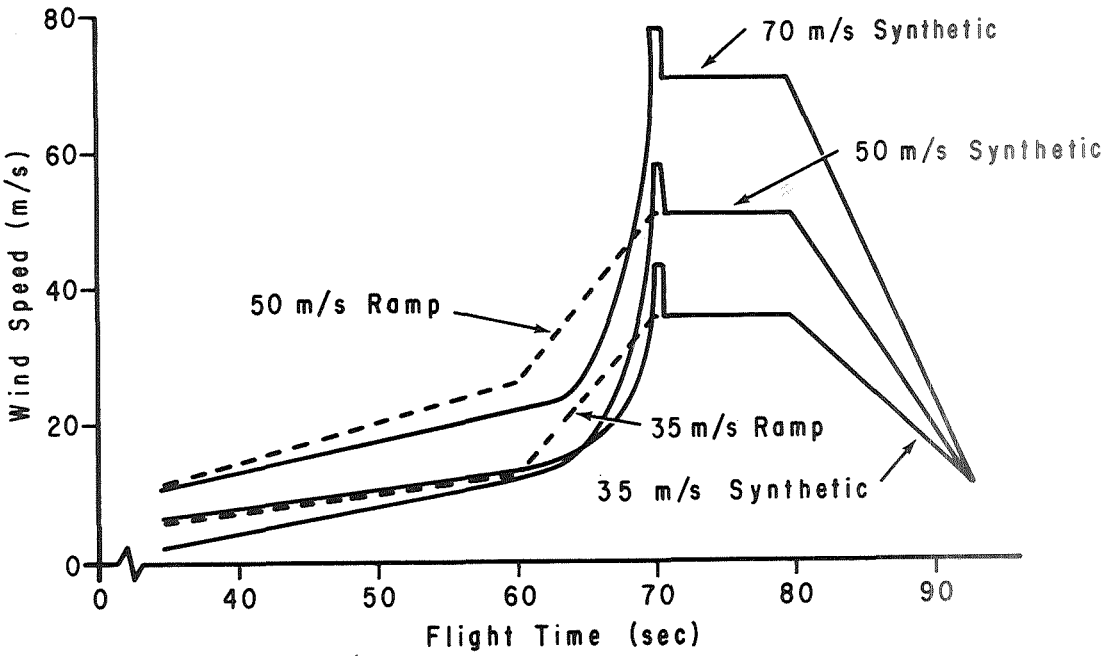

Figure 7. Comparison of Ramp Wind Profiles with Synthetic Wind Profiles Peaking at 10 km

Figure 8 compares the wind restriction for the 35 m/s synthetic and the 35 and 50 m/s ramp wind bias steering commands which were 63.0, 68.7 and 78.7 m/s, respectively. The 50 m/s ramp wind bias steering command provided 15.7 m/s more capability than the synthetic and 20.7 m/s more capability than the mean wind bias steering commands. Only the maximum wind speed capability was determined for these steering commands and no attempt was made to investigate the minimum wind speed capability. The ramp wind bias steering commands as seen in figure 9 are composed of six distinct setments as follows:

(a) Initial steering ledge.

(b) Discontinuity.

(c) Initial shear buildup.

(d) Final shear buildup.

(e) Steady state wind speed.

(f) Shear backoff.

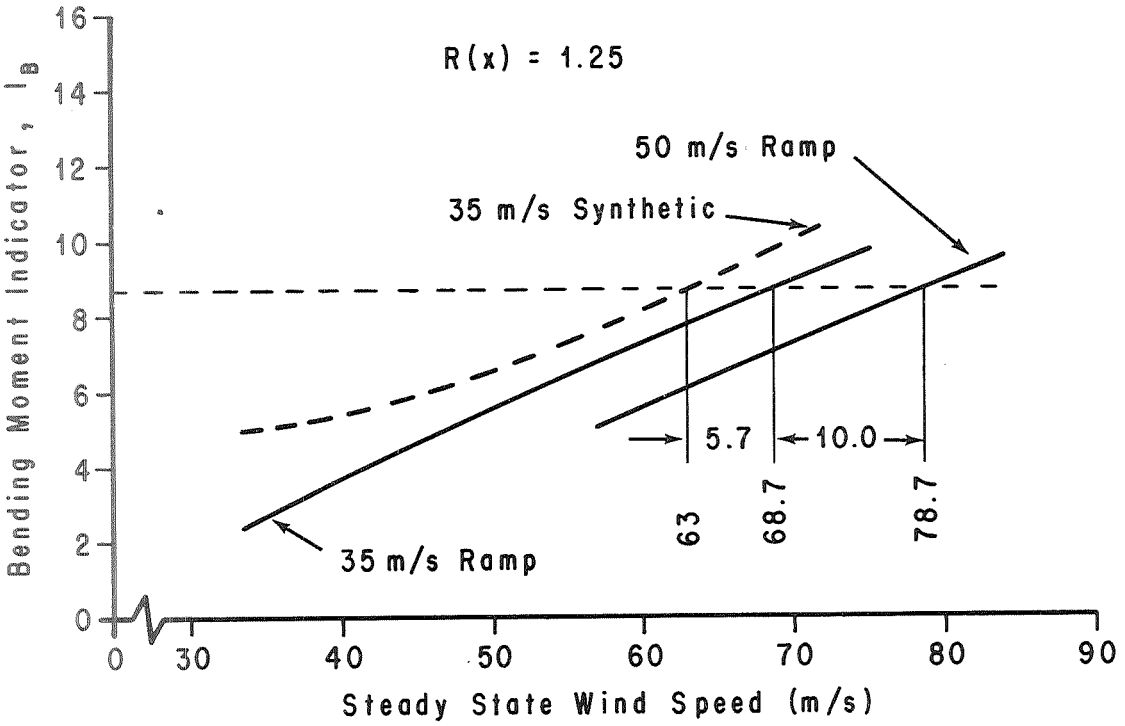

Figure 8. Wind Restriction for Yaw Bias to 35 m/s Synthetic and 35 m/s and 50 m/s Ramp Winds Peaking at 10 km

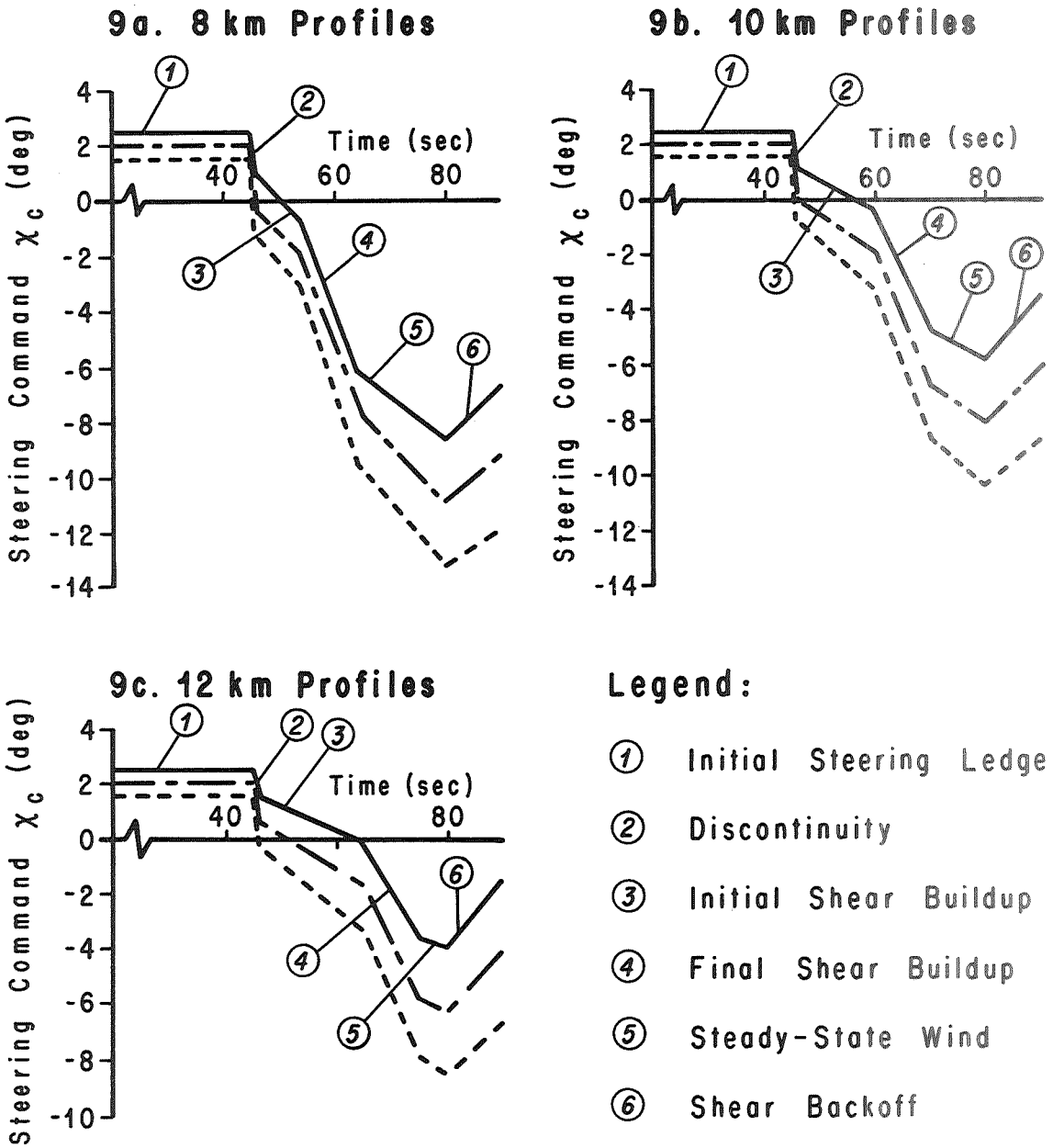

Figure 9. Yaw Steering Profiles for 50 m/s Ramp Wind Profiles Peaking at 8, 10 and 12 km with Variations in Initial Steering Ledge

The initial steering ledge is used to build up drift before max q. As the dynamic pressure builds up, the steering logic is changed to command the vehicle to fly a zero angle-of-attack trajectory, resulting in a discontinuity in the steering command. In actual practice, segment 1 would be gradually blended into segment 3. Segments 3 through 6 result from commanding the vehicle to fly zero angle-of-attack along the initial and final shear buildup, steady-state wind speed, and shear backoff.

3. Effect of Initial Ledge Command

To evaluate the effect of the initial ledge of the steering command profile, a series of bias steering commands was generated for ramp winds peaking at 8, 10 and 12 km by varying the initial steering ledge from 1.5 to 2.5 degrees. As previously mentioned, the initial ledge is used to enable the vehicle to build up an initial drift rate by turning the vehicle with the wind during the early part of boost flight. As the dynamic pressure rises, producing increased aerodynamic loading, the vehicle is commanded to follow a zero angle-of-attack trajectory. The point at which one stops building up drift and begins to fly zero angle-of-attack is somewhat arbitrary; 45 seconds was chosen to correspond to the Skylab 6-D trajectory. The steering profiles are shown in figures 9a, 9b, and 9c for the 8, 10, and 12 km profiles, respectively.

The most distinctive feature of these ramp wind-bias steering profiles is that the profiles have constant slope changes at points corresponding to the changes in the slope of the biasing wind profile (except for the initial discontinuity at 45 sec). This feature minimizes the computer storage requirements for defining the shape of the steering command in simulations and in actual flight hardware. Another characteristic is that each family of profiles indicated negligible differences in angle of attack and bending moment indicator I_b when subjected to a 70 m/sec synthetic wind. This would tend to indicate that the turning rate for each profile is optimum for the amount of drift set up by the initial steering ramp.

However, each of the families proved to be optimum only at the altitude for which the biasing wind peaked. In general, the 10 km bias profiles yielded the best results (see figure 10). The 8 km profile yielded about the same results as the 10 km profile in response to a 70 m/s wind at 8 km. This tends to indicate that the analyst can initially concentrate on the most critical altitude (10 km in this case), and seek improvement at lower and higher altitudes at a later date if it is required.

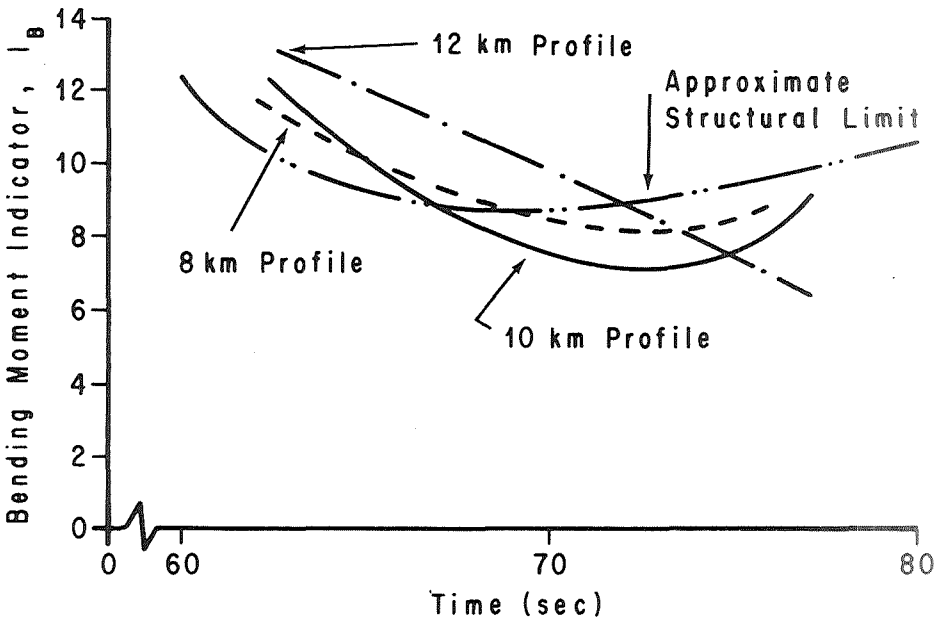

Figure 10. Bending Moment Indicator for 8, 10 and 12 km Bias Profiles in Response to a 70 m/s Synthetic Wind

The methods by which structural loads can be minimized in the max q region have been discussed in some detail. The question now arises "What are the real tradeoffs between the methods?" The initial parameter encountered in this study was terminal drift. Since in a guidance scheme it is necessary to minimize or control terminal drift, some scheme must be built into the trajectory shaping to accomplish this feat.

By using drift rate to minimize angle of attack, one ends up with a large terminal drift rate in one direction (positive in this model), and turning into the wind produces a large drift rate in the opposite direction. By a proper combination of the two techniques, the drift rate can be minimized at any time of interest. Figure 11 shows the effect on terminal drift rate of varying the initial ledge of the steering profile. This figure also shows the drift rates at 90 sec obtained by varying the ledge from 1.5 to 2.5 degrees, and indicates that, for sufficient increases in the initial steering ledge, the drift rate at 90 sec can be set to zero. Alternately, the drift rate could be set to any desired value.

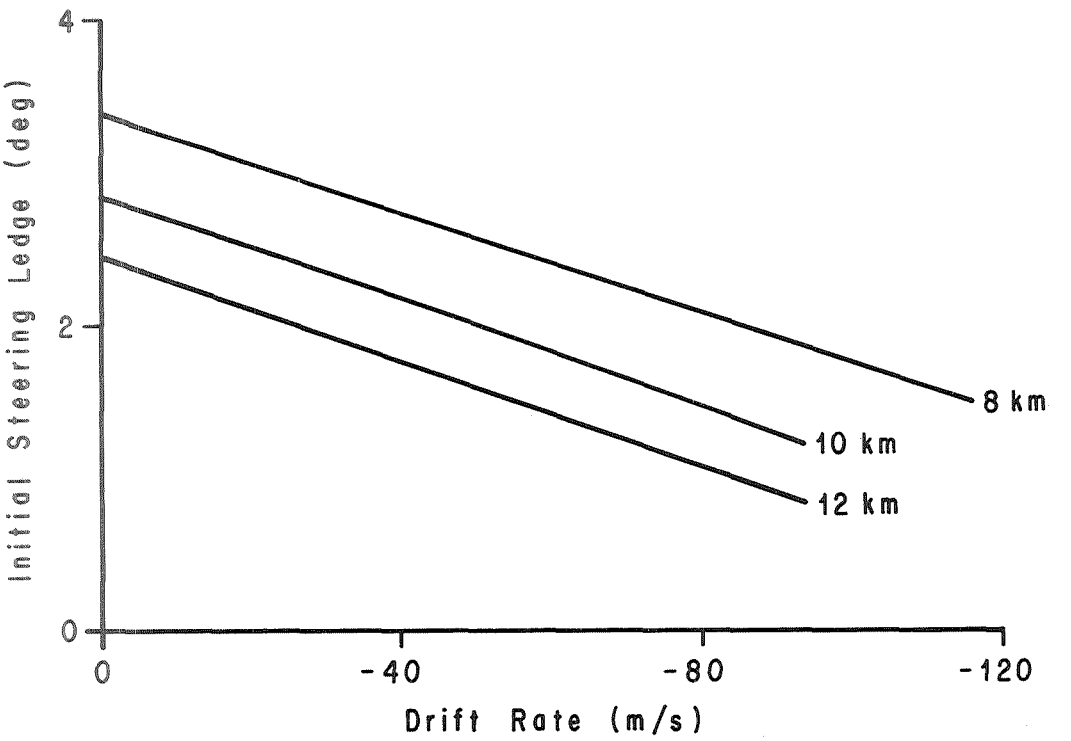

Figure 11. Effect of Initial Steering Ledge on Drift Rate at 90 Seconds for 50 m/s Ramp Winds Peaking at 8, 10 and 12 km

4. Limiting Factors for Biasing

Figure 12 shows the effect of the initial steering ledge on the maximum turning angle required to produce zero angle of attack in the presence of the biasing wind. Although this variation has little importance in terms of wind response, it may have some bearing on steering logic for engine out or abort studies where one might fly a frozen command for an extended period of time and thereby set up excessive terminal drift.

While attempting to improve the vehicle response to large wind magnitudes, one should also address the problem of response to minimum wind speed or winds from a counter-direction. The steering profiles generated for the 50 m/s ramp wind indicated sufficient structural margins in the no-wind case. Since the low wind speeds have correspondingly low shears, biasing the trajectory for the low or no-wind case could provide a limiting case for maximizing the peak-wind case.

Figure 13 shows the steering profile used to generate a -6° (negative) angle of attack at 10 km for the no-wind case. Also shown are the angle-of-attack responses for no-wind and for 70 m/sec synthetic wind profiles peaking at 8, 10, and 12 km. Figure 14 shows the bending moment indicator for these four cases compared with the approximate

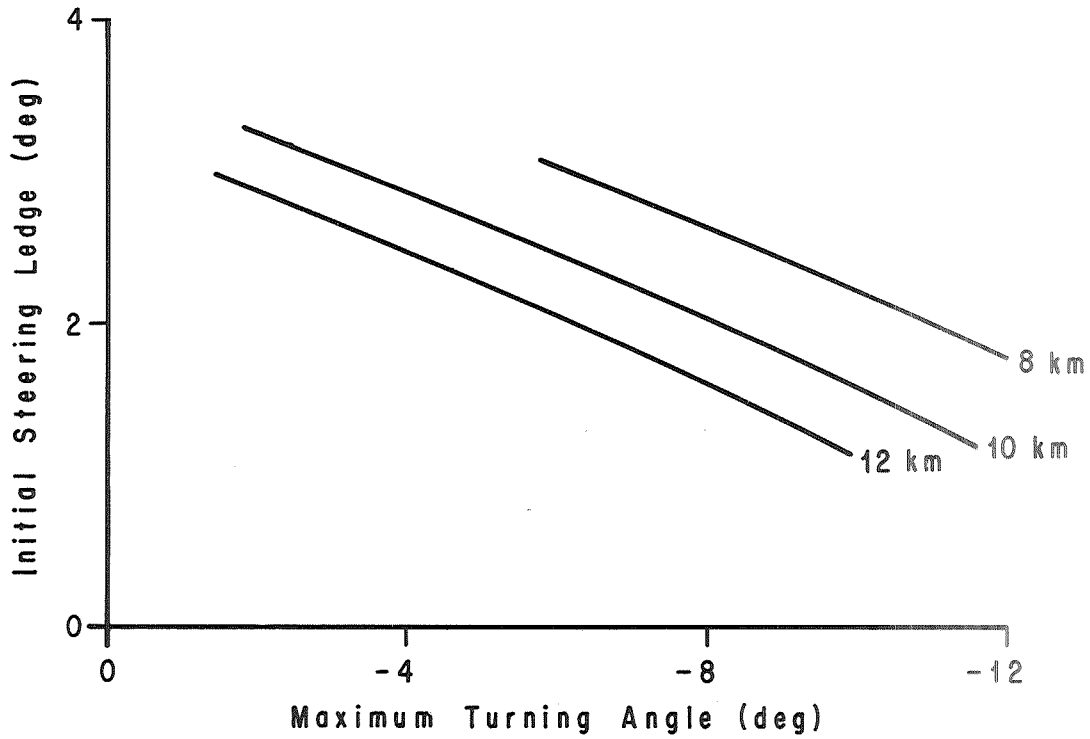

Figure 12. Effect of Initial Steering Ramp on Maximum Turning Angle Required to Produce Zero Angle of Attack During Max Q for 50 m/s Ramp Winds Peaking at 8, 10 and 12 km

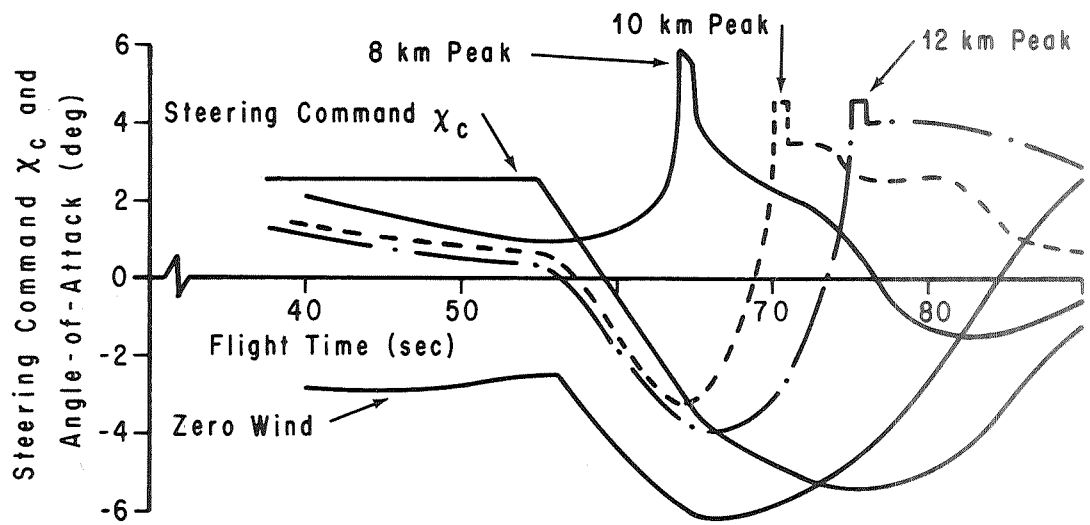

Figure 13. Zero-Wind Angle-of-Attack Steering Command and Response to Synthetic Wind Profiles

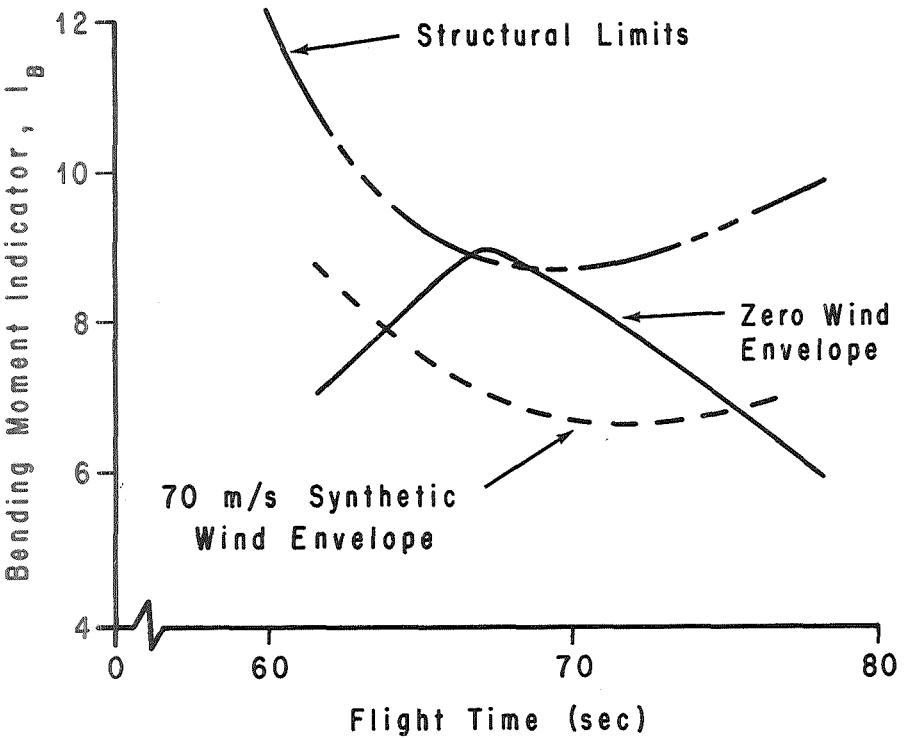

Figure 14. Bending Moment Indicator for Zero-Wind Angle-of-Attack Steering Command for Zero Wind and 70 m/s Wind Peaking at 8, 10 and 12 km.

structural limit. This profile yielded the best response characteristics to the synthetic winds, but at the incurred penalty of obtaining high bending moments in the no-wind case.

We have shown various yaw plane biases and indicated that the trends can be applied to the pitch plane. Biasing simultaneously in pitch and yaw will be done for the present Skylab flight azimuth. When one accounts for the probability of large winds occurring in either plane, the effects must be considered jointly. If the vehicle must withstand equal wind magnitudes from two directions independently (or simultaneously), this provides a limit on the amount of biasing that can be done independently in the two planes. If biasing to the mean wind is not sufficient, the next step would be to use real-time biasing based on the statistics of wind persistence in both direction and magnitude. Alternately, a family of bias profiles could be generated to encompass the probable combination which might be encountered.

Other attempts at improving the overall wind limits included combining several biasing profiles by least squares and weighting techniques. The profiles investigated in the optimization were those corresponding to the 2.5° initial steering ramp profiles of figure 9. However, none of these methods provided a steering profile which was as good as the 10 km bias profile (data not presented).

IV. SIMULATION RESULTS

To facilitate a realistic assessment of launch probability, a high-speed six-degree-of-freedom simulation program was developed for use on a hybrid computer. This program contains the following features:

(1) First stage trajectory flight simulation.

(2) Closed-loop control with three-axis steering.

(3) Two elastic body modes.

(4) Control filter network and second-order actuator models.

(5) Wind data input via magnetic tape (Jimsphere profiles) or cards (synthetic profiles).

(6) Speed of 20 times real time.

(7) Bending moment calculation at three vehicle stations.

(8) Discrete level sensing of five parameters at four-second intervals.

(9) Maximum value sampling of five parameters in each four-second interval.

(10) Calculation of statistics of data and exceedance of discrete levels.

(11) Identification of wind profiles producing exceedances.

A selection of approximately 1200 Jimsphere wind profiles from the Eastern Test Range sampled over a three-year period was available for the initial investigation. These data, recorded on magnetic tape, contain wind speed and direction at 25-meter increments up to an altitude of 16-18 km. Use of these profiles in the simulation allows a direct determination of launch probability because they account for the correction between windspeed, direction, shear, and gust. These profiles do not provide wind limits.

To evaluate the effectiveness of wind biasing, the launch probability was evaluated for the nominal and biased trajectories. Bending moments were calculated for critical vehicle stations, and the probability of not exceeding the structural capability was determined. This probability then becomes the launch probability. Then any increase in launch probability due to inclusion of a bias will indicate the effectiveness of the bias. In the actual monthly samples analyzed thus far, the increase in launch probability was substantial.

Data for five parameters (α, β, and three bending moments) were sampled every four seconds in the interval from 50 to 90 seconds of vehicle flight. These data, along with the maximum values in each four-second interval, were analyzed to obtain the timewise distribution of each parameter in terms of its mean and variance. In addition, the maximum value of each parameter for each run was obtained to give an overall distribution which would readily show trends.

The data were fitted by a distribution function which was then used in plotting the results. Figures 15 and 16 contain results obtained from the March wind sample. Distributions for the 50-90 second interval are shown for α, β, and M_B (80). It can be seen that wind biasing has considerably reduced the vehicle loads and the probability of a launch delay.

Figure 17 presents the timewise distribution of vehicle bending moment M_B (80). This figure was obtained from the Cumulative Probability Frequency (CPF) of the measured data. The curves labeled maximum envelope represent the largest measured value in each interval. Superimposed on this figure is an approximation of the maximum allowable bending moment for this station. Again it can be seen that the probability of not encountering a launch delay is greater than 95% but less than 100% for the mean wind biased trajectory. To provide correlation with launch probabilities obtained by the synthetic wind approach, data obtained from the months of November, January, February and March are compared in table II. These data are given as launch probability or the probability of not encountering a launch delay due to winds. The bias trajectory analyzed was developed for March, and no attempt was made to obtain a biased trajectory developed using the monthly means for the other months. However, there is only a small difference in the January through March monthly means. The results should correctly be interpreted as showing that the launch probability can be increased by biasing to some given wind profile.

Table II. Probability of Not Encountering A Launch Delay Due to Wind

	Synthetic Wind		Jimsphere Wind	
Month	Unbiased	Biased	Unbiased	Biased
November	58%	96%	88%	97%
January	27%	92%	80%	98%
February	28%	90%	70%	98%
March	26%	90%	64%	97%

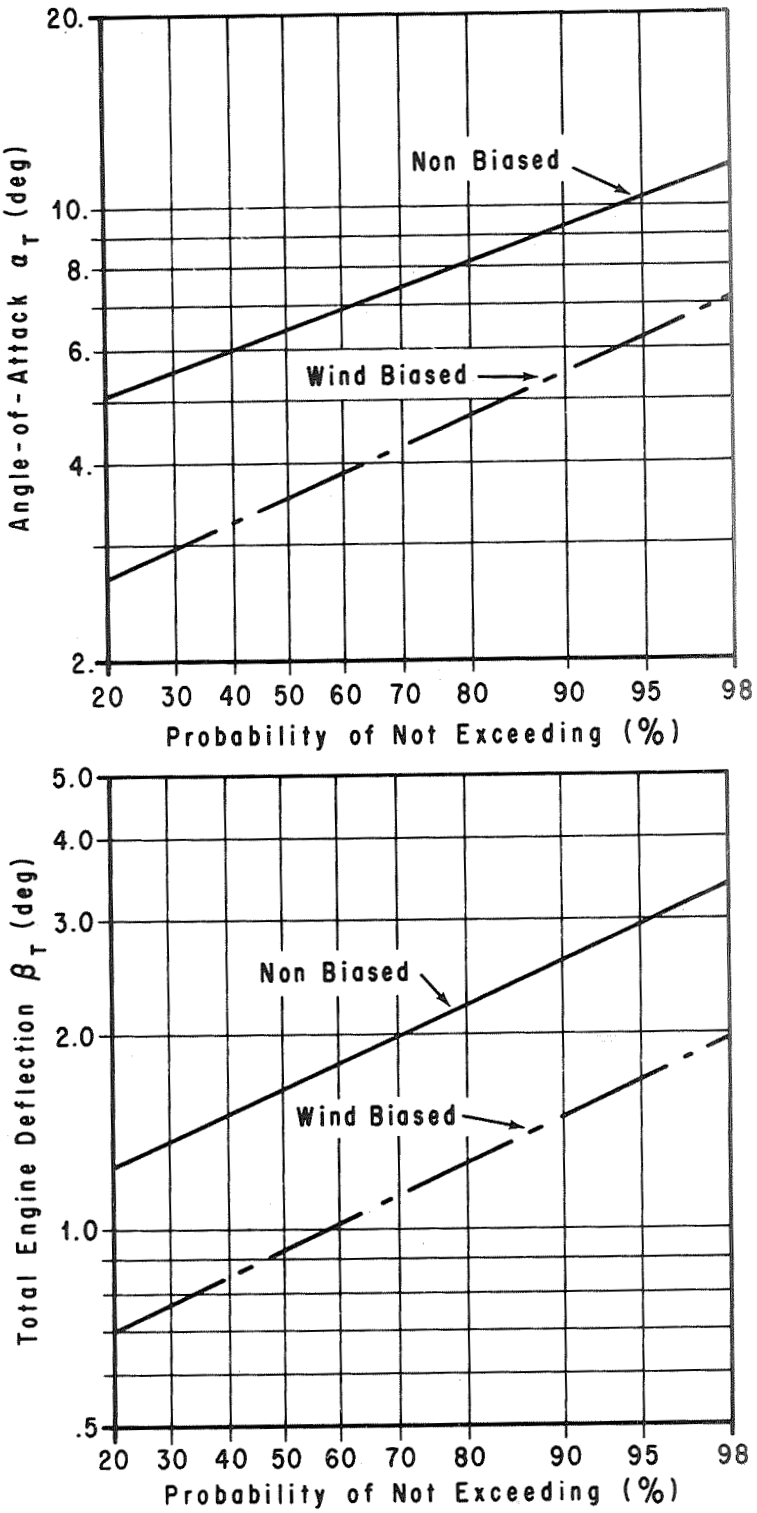

Figure 15. Total Angle of Attack (α_T) and Total Deflection (β_T) vs the Probability of Not Exceeding for March Sample of Jimsphere Winds

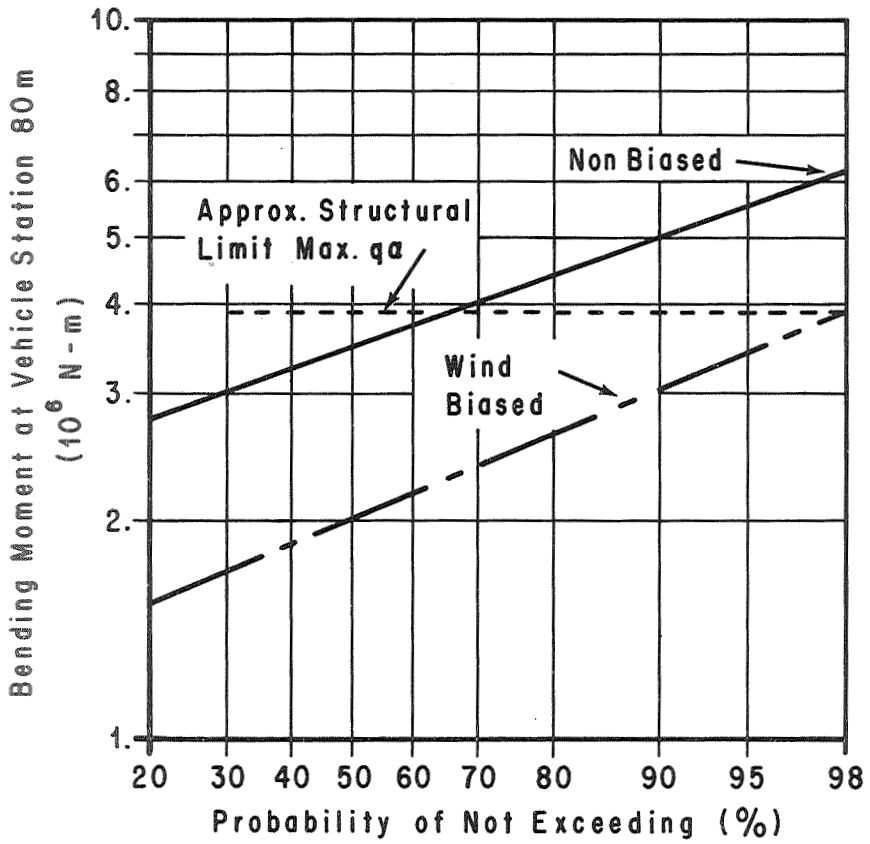

Figure 16. Maximum Bending Moment at Vehicle Station 80 Meters vs Probability of Not Exceeding for March Sample of Jimsphere Winds

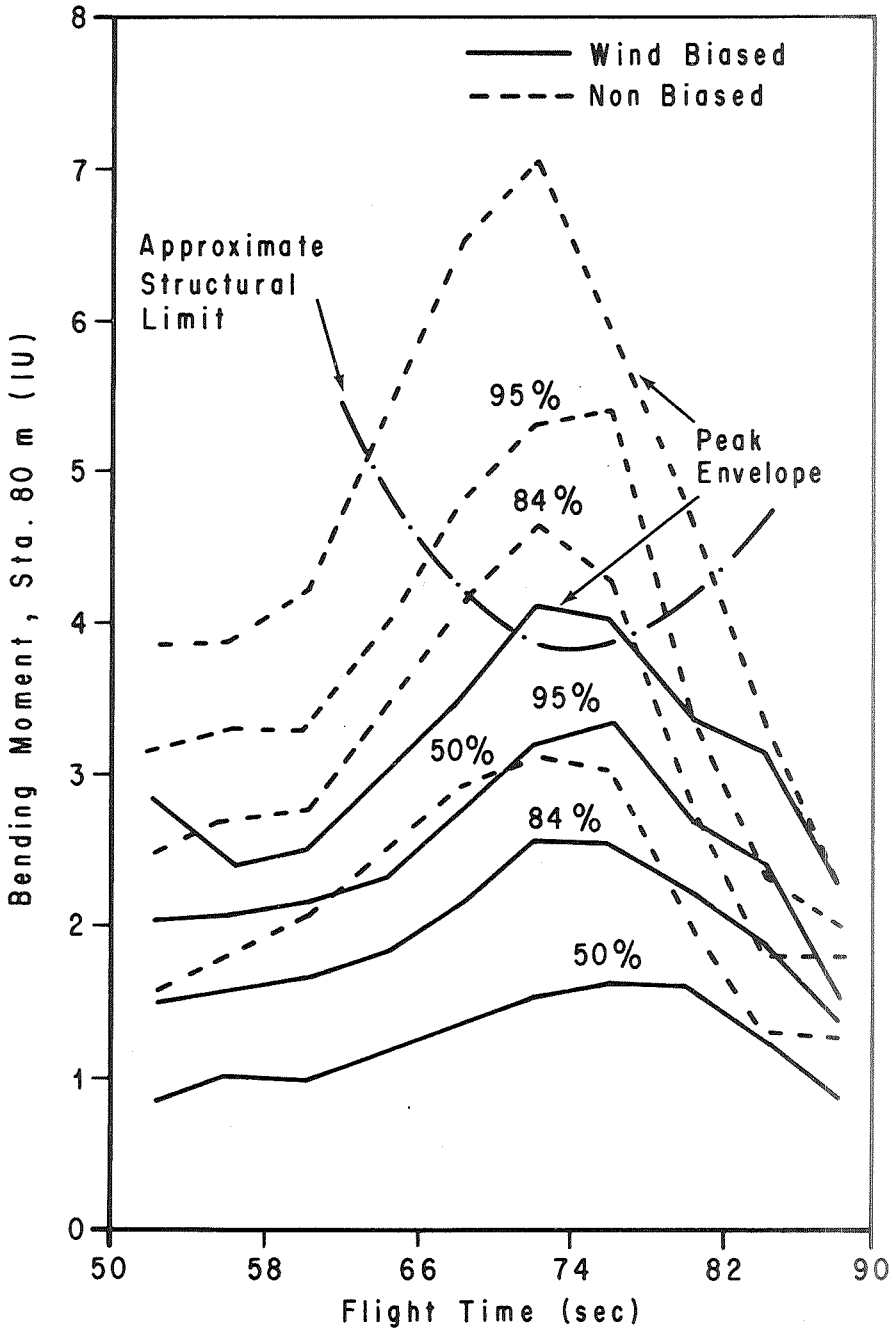

Figure 17. Skylab Bending Moment Profiles Using March Jimsphere Wind Sample

The results contained in table II show a substantial increase in launch probability for the unbiased trajectory when the Jimsphere wind profiles were used instead of synthetic profiles. The increase in launch probability for the bias trajectory comparison, although not so dramatic, is still significant. The results for the unbiased trajectory comparison indicate that the synthetic winds are overly conservative for this vehicle configuration and that the probability of encountering a 95% steady-state wind speed with 99% shears and gusts [1] is extremely small. Studies conducted on the Saturn V launch vehicle configuration showed agreement between the synthetic and Jimsphere wind profiles for the unbiased case using attitude control only. However, the synthetic wind profile indicated a 20% reduction in bending moment using a load relief control scheme, while the Jimsphere profiles showed only a 5% reduction. In this instance, the synthetic profile was not conservative, and gave more of a risk.

V. CONCLUSIONS AND RECOMMENDATIONS

It has been generally demonstrated in the preceding sections how wind biasing can be used to increase launch opportunity during months with a high probability of large wind magnitudes (with an associated direction) and high wind shears. Three methods of performing the bias were mentioned: (1) continuously turning into the wind ($\varphi = -V_W/V$), (2) canceling the wind with drift velocity ($\dot{Y} = V_W$), and (3) a combination of the first two methods ($\varphi = (\dot{Y}-V_W)/V$). Method (3) was selected as the best method for this study in that it offered the best means of controlling terminal drift and drift rate. This method has been successfully used on Saturn vehicles and has been effective even in load relief control systems (Saturn I and IB).

In using method 3, an initial drift rate was established with the initial steering ledge; and as the dynamic pressure built up, the vehicle was commanded to fly a zero angle-of-attack trajectory. During this portion of the trajectory, the biasing wind is balanced with a combination of drift rate and turning into the wind to produce zero angle of attack. It was also indicated that the two portions of the trajectory should be blended to eliminate any discontinuity or transient vehicle response. In section III, it was shown that the terminal drift and drift rate could be controlled by varying the initial steering ledge. It was concluded that this was the major influence of the initial steering ledge.

Section III also showed that biasing wind profiles other than the mean wind could be used in generating the bias steering command. The best of these profiles seemed to be the ramp wind profile which could be

simply constructed and the resulting bias steering command was composed of straight line segments.

The limiting factor in biasing to large wind magnitudes was the possibility of encountering winds of opposite direction to the biasing wind and winds normal to the plane of the bias. As an extreme example, a bias steering command was generated to give a large negative angle of attack (see figures 13 and 14) with zero wind velocity. In this example, the vehicle capability was shown to be in excess of 70 m/s, but for zero wind the structural limit was slightly exceeded at about 68 seconds.

The conclusion drawn from this part of the study was that biasing the trajectory using wind profiles other than a monthly mean should be carefully weighed against the available wind statistics for the month(s) of launch. The recommended procedure for developing a wind biased trajectory is to use the mean wind vector for the month of launch and develop a steering command as outlined in method 3 above. Other choices exist where launch may take place during a period covering more than one month. During the January through March period, there is no significant difference in the statistics, and a bias based on March statistics will adequately cover all three months. During other monthly periods, it has proved expedient and satisfactory to develop a bias using the mean wind vector averaged over the period of interest. These outlined procedures have all been successfully used in developing bias trajectories at MSFC.

The other types of wind profiles mentioned in this study are recommended for use only after careful analysis of the bias using the mean wind vector and the biasing function has shown that the probability of a successful launch is not acceptable. The next logical step would be to use a ramp-type profile to reach the peak wind speed of the components of the mean vector wind. A high speed detail wind simulation as outlined in this report could be used to determine which plane (pitch or yaw) needed enhancement to increase launch probability.

Care should also be used in using wind statistics in assessing launch risk. The capability to withstand the 95% envelope of wind speed (with associated shears and gusts) does not imply a 95% chance of successful launch. It is possible to have a different 5% of the total population of winds exceeding the vehicle's wind capability at each altitude interval, resulting in a launch probability considerably below 95%. For this reason the counting procedure outlined in section II is used.

A standard procedure has been set up at MSFC to determine launch probability and preclude vehicle loss due to high altitude winds. The procedure is summarized as follows:

(1) Establish wind speed limits versus altitude.

(2) Determine the probability of a successful launch.

(3) If the probability is not acceptable, formulate a mean wind biasing trajectory.

(4) Determine the wind limits and probability of a successful launch.

(5) Establish a prelaunch wind monitoring and simulation capability using winds measured within 8 hours or less of the launch.

In addition to the above procedure, the MSFC high-speed simulation will be used to predict the launch probability directly using selections of the Jimsphere profiles for each month. The number of wind profiles which cause bending moments greater than the structural capability will be counted and the result used to determine the probability of success. This will give the true launch probability for a representative selection of winds. The synthetic wind approach which is used in steps 1 through 4 above will only give a scalar "conditional" probability statement.

The advantage of a high-speed analog or hybrid simulation program is that it allows a large number of detailed wind profiles to be examined in a short amount of time. At a speed of 20 times real time, 90 seconds of vehicle flight through a sample of 135 wind profiles can be obtained in approximately 12 minutes. Wind profiles of particular interest can be analyzed in more detail on a digital program and avoid the time-consuming effort of looking at all of the profiles digitally. By storing parameters of interest on magnetic tape, one can identify the wind profile producing large angle of attack, bending moment, etc.

Another advantage to high-speed simulations with real wind profiles would be gain scheduling within prescribed stability limits to determine the most effective gains with and without wind biasing. Similarly, the effects of vehicle data uncertainties such as c.g. offsets, engine misalignments, etc., can be assessed using Monte Carlo techniques. Recent studies on the Skylab indicated a 20% increase in the mean bending moment, but only a 6% increase in the mean $+2\sigma$ level. The net effect on launch probability was negligible for the wind biased trajectory. The implications of these results are not yet fully understood and a different approach to the problem (using the "A" factor method) is being implemented. This should give a conservative estimate of the bending moment distribution to compare with the Monte Carlo results.

Further areas of investigation which are recommended for consideration with the MSFC high-speed simulation program are

(1) bias optimization,

(2) control gain optimization,

(3) error analysis for both biased and nonbiased trajectories,

(4) method of estimating bias effectiveness without generating bias trajectory,

(5) correlation of detailed wind results with synthetic wind results,

(6) correlation of detailed wind results with joint wind speed/wind shear statistics, and

(7) correlation of detailed wind results with random wind models.

REFERENCES

1. Daniels, Glenn E., editor, "Terrestrial Environment (Climatic) Criteria Guidelines for Use in Space Vehicle Development, 1969 Revision," NASA TM X-53872, MSFC, September 8, 1969; March 15, 1970 (Second Printing).

2. Smith, O. E., "An Application of Distributions Derived from the Bivariate Normal Density Function," published as part of proceedings of the International Symposium on Probability and Statistics in the Atmospheric Sciences, Honolulu, Hawaii, June 1971.

3. Lovingood, J. A., "A Technique for Including the Effects of Vehicle Parameter Variations in Wind Response Studies," NASA TM X-53042, MSFC, May 1, 1964.

APPROVAL

WIND BIASING TECHNIQUES FOR USE IN OBTAINING LOAD RELIEF

by Gale Ernsberger

The information in this report has been reviewed for security classification. Review of any information concerning Department of Defense or Atomic Energy Commission programs has been made by the MSFC Security Classification Officer. This report, in its entirety, has been determined to be unclassified.

This document has also been reviewed and approved for technical accuracy.

Paul T. Craighead

P. T. Craighead
Chief, Control Development Section

R. S. Ryan
Chief, Flight Analysis Branch

for J. A. Lovingood
Chief, Dynamics and Control Division

for E. D. Geissler
Director, Aero-Astrodynamics Laboratory

MSFC—RSA, Ala

DISTRIBUTION

DIR
DEP-T
A&TS-PAT
PM-PR-M, Mr. Goldston
A&TS-MS-H
A&TS-MS-IP
A&TS-MS-IL (8)
A&TS-TU, Mr. Wiggins (6)

PM
- Mr. Smith
- Mr. Bell
- Mr. McCulloch
- Mr. Belew
- Mr. Hardy
- Mr. Kurtz

S&E-ASTR
- Mr. Moore
- Mr. Wojtalik
- Mr. Scofield
- Mr. Vallely

S&E-ASTN
- Mr. Heimburg
- Mr. Sterett
- Mr. Hunt
- Mr. McCool
- Mr. Platt
- Mr. Isbell
- Mr. Stevens
- Mr. Kroll
- Mr. Farrow
- Mr. Frederick
- Mr. Moore

S&E-CSE
- Mr. May

S&E-P
- Mr. Vreuls

S&E-COMP
- Dr. Hoelzer
- Mr. Prince
- Mr. Rich

S&E-AERO
- Dr. Geissler
- Mr. Horn
- Dr. Lovingood
- Mr. Ryan
- Mr. Mowery
- Mr. Craighead
- Mr. Rheinfurth
- Mr. Lindberg
- Mr. Cremin
- Mr. Hardage
- Mr. Sims
- Mr. Jackson
- Mr. Dahm
- Mr. Vaughan
- Mr. Kaufman
- Mr. Smith
- Mr. Baker
- Mr. Ernsberger (20)
- Mrs. Hightower

Sci. & Tech. Info. Facility (25)
P. O. Box 33
College Park, Md. 20740
Attn: NASA Rep. (S-AK/RKT)

NASA-Lewis Research Center
Cleveland, Ohio 44135
Attn: Mr. Gerus, Mail Stop 62

NASA-Langley Research Center
Hampton, Va. 23365
Attn: Mr. Runyan, Mail Stop 242
Mr. Morgan, Mail Stop 242
Mr. Love, Mail Stop 412

NASA-Manned Spacecraft Center
Houston, Texas 77001
Attn: Mr. Cline, BMS
Mr. Mackey, ES2
Mr. Frasier, EG
Mr. Chilton, EG
Mr. Cheatham, EG
Mr. Gilbert, EG6
Mr. Kennedy, EG13
Mr. Thomas, EX2
Mr. Wade, ES2
Mr. Schwartz, ES2

Northrop Corp.
Electro-Mech. Div.
P. O. Box 1484
Huntsville, Ala. 35807
Attn: Mr. Sloan
Mr. Echols

NASA-Ames Research Center
Moffett Field, CA 94035
Attn: Mr. Creer

NASA Hdqs.
Washington, DC 20546
Attn: Mr. Michaels, REG
Mr. Janow, REG
Mr. Carley, MHE

NASA-Flight Research Center
P. O. Box 273
Edwards, CA 93523
Attn: Mr. Gee, R
Mr. Layton, R

NASA-Kennedy Spacecraft Center
Kennedy Space Center, Fla. 32931

Convair Airspace Div.
General Dynamics Corp.
P. O. Box 1128
San Diego, CA 92112
Attn: G. R. Friedman, Mail Zone 585-00
A. W. Nelson, Mail Zone 585-00